ACS APPLIED MATERIALS & INTERFACES

www.acsami.org

Research Article

Flagellin/Virus-like Particle Hybrid Platform with High Immunogenicity, Safety, and Versatility for Vaccine Development

Yiwen Zhao, Zhuofan Li, Jewel Voyer, Yibo Li, and Xinyuan Chen*

Cite This: https://doi.org/10.1021/acsami.2c01028

Read Online

ACCESS | Metrics & More | Article Recommendations | Supporting Information

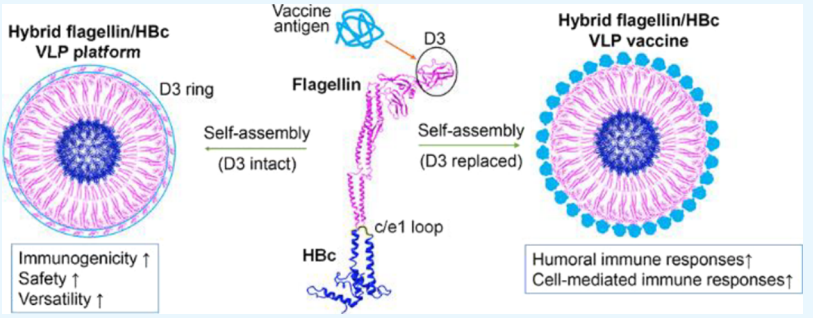

ABSTRACT: Hepatitis B core (HBc) virus-like particles (VLPs) and flagellin are highly immunogenic and widely explored vaccine delivery platforms. Yet, HBc VLPs mainly allow the insertion of relatively short antigenic epitopes into the immunodominant c/e1 loop without affecting VLP assembly, and flagellin-based vaccines carry the risk of inducing systemic adverse reactions. This study explored a hybrid flagellin/HBc VLP (FH VLP) platform to present heterologous antigens by replacing the surface-exposed D3 domain of flagellin. FH VLPs were prepared by the insertion of flagellin gene into the c/e1 loop of HBc, followed by *E. coli* expression, purification, and self-assembly into VLPs. Using the ectodomain of influenza matrix protein 2 (M2e) and ovalbumin (OVA) as models, we found that the D3 domain of flagellin could be replaced with four tandem copies of M2e or the cytotoxic T lymphocyte (CTL) epitope of OVA without interfering with the FH VLP assembly, while the insertion of four tandem copies of M2e into the c/e1 loop of HBc disrupted the VLP assembly. FH VLP-based M2e vaccine elicited potent anti-M2e antibody responses and conferred significant protection against multiple influenza A viral strains, while FljB- or HBc-based M2e vaccine failed to elicit significant protection. FH VLP-based OVA peptide vaccine elicited more potent CTL responses and protection against OVA-expressing lymphoma or melanoma challenges than FljB- or HBc-based OVA peptide vaccine. FH VLP-based vaccines showed a good systemic safety, while flagellin-based vaccines significantly increased serum interleukin 6 and tumor necrosis factor α levels and also rectal temperature at increased doses. We further found that the incorporation of a clinical CpG 1018 adjuvant could enhance the efficacy of FH VLP-based vaccines. Our data support FH VLPs to be a highly immunogenic, safe, and versatile platform for vaccine development to elicit potent humoral and cellular immune responses.

KEYWORDS: *flagellin, HBc, VLP, M2e, universal influenza vaccine, CpG 1018, cancer vaccine, CTL*

INTRODUCTION

Vaccine development focuses more and more on individual antigens and T and B cell epitopes rather than whole pathogens. This targeted approach avoids adverse reactions caused by irrelevant components of pathogens and significantly improves the vaccine safety. Yet, proteins and antigenic epitopes often have low immunogenicity due to their inefficient uptake by dendritic cells (DCs) and weak stimulation of DC maturation. The linkage of protein antigens or antigenic epitopes to vaccine delivery platforms can significantly improve vaccine immunogenicity.

Virus-like particles (VLPs) are highly immunogenic vaccine delivery platforms. VLPs can be efficiently taken up by DCs, presented on major histocompatibility complex class I and II molecules, and elicit humoral and cell-mediated immune responses simultaneously.[1−3] VLP-based hepatitis B and human papillomavirus vaccines have been approved for human use.[1,2] VLPs can also be engineered to display foreign antigenic epitopes. This can be achieved by the insertion of antigenic epitopes to N- or C-termini or specific internal regions of viral capsid proteins, followed by their self-assembly into VLPs. One successful example is malaria RTS,S vaccine (Mosquirix), which was developed based on the self-assembly

Received: January 17, 2022
Accepted: April 13, 2022

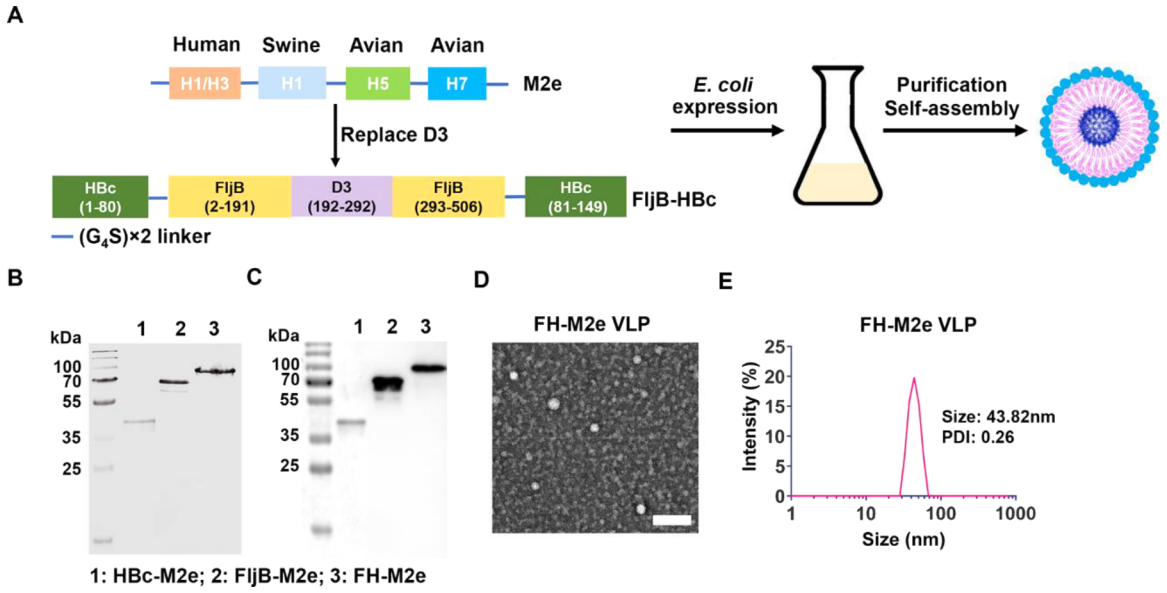

Figure 1. FH VLP-based M2e vaccine design and characterization. (A) Schematic illustration of FH VLP-based M2e vaccine design and preparation. (B,C) Purified HBc-M2e, FljB-M2e, and FH-M2e fusion proteins were subjected to SDS-PAGE (B) and western blotting analysis (C). Immune sera collected from KLH-M2e-immunized mice were used in western blotting analysis. (D) TEM analysis of FH-M2e VLPs. Scale: 100 nm. (E) DLS analysis of FH-M2e VLPs in Zetasizer Nano ZS (Malvern). PDI: polydispersity index.

of native and chimeric hepatitis B surface antigen (HBsAg) at approximately 3:1 molar ratio.[4] Chimeric HBsAg contains an immunodominant repetitive epitope of the circumsporozoite protein of *Plasmodium falciparum* inserted to its N-terminus.[5]

Hepatitis b core (HBc) VLPs represent one of the most explored VLP platforms for foreign antigen display.[6] The major immunodominant region of HBc (c/e1 loop) presents an ideal site for the insertion of antigenic epitopes to display on the VLP surface. Antigenic epitopes from a variety of viral and bacterial pathogens have been successfully displayed on the HBc VLP surface and showed significantly improved immunogenicity in preclinical studies.[7] HBc VLPs displaying the circumsporozoite epitopes of *Plasmodium falciparum* have been tested in clinical trials.[8,9] Yet, the c/e1 loop of HBc mainly allows the insertion of relatively short antigenic epitopes to not affect the VLP assembly.[10,11]

Besides VLPs, highly immunogenic proteins have also been explored as vaccine delivery platforms. Flagellin is the major component of bacterial flagellum and a potent toll-like receptor (TLR) 5 agonist. Flagellin has been extensively explored as a highly immunogenic carrier for vaccine development against bacterial, viral, and parasitic diseases.[12,13] Flagellin contains highly conserved D0 and D1 domains and variable D2 and D3 domains.[14] D1 domain is responsible for TLR5 activation,[14] while D3 domain can be replaced with relatively long antigenic epitopes without affecting the TLR5 activation.[15−17] Vaccine antigens can also be inserted to its N- or C-terminus to develop recombinant vaccines. Several flagellin-based vaccines have advanced to clinical trials.[18−21] Despite their good immunogenicity, flagellin-based vaccines carry the risk of inducing systemic adverse reactions, especially at high doses, due to the overactivation of TLR5.[18−21]

Recently, we developed a hybrid flagellin/HBc VLP (FH VLP) platform, in which FljB (phase 2 flagellin of *Salmonella typhimurium strain LT2*) was displayed on the HBc VLP surface at a 1:1 FljB-to-HBc molar ratio via c/e1 loop insertion.[22] Due to the closely juxtaposed N- and C-termini of FljB, insertion of relatively big FljB (505 aa) did not affect the self-assembly of HBc VLPs. FH VLPs stimulated strong DC maturation without the induction of systemic cytokine release.[22] FH VLPs were found to serve as a more immunogenic carrier for nicotine vaccine development as compared to FljB and HBc VLPs.[22]

FH VLPs are expected to also serve as a highly immunogenic and safe platform for recombinant vaccine development by replacing the surface-exposed D3 domain of FljB. This study explored FH VLPs for the ectodomain of matrix protein 2 (M2e)-based universal influenza vaccine development and cytotoxic T lymphocyte (CTL) epitope of ovalbumin (OVA)-based tumor vaccine development. The exploration of both allows us to evaluate the ability of FH VLPs to elicit protective humoral- and cell-mediated immune responses against surface-displayed vaccine antigens.

RESULTS

Generation and Characterization of FH-M2e VLPs. M2e is an attractive target for universal influenza vaccine development due to its high-sequence homology among influenza A viruses.[23] A large body of evidence supports the cross-protective immunity of anti-M2e antibodies via diverse mechanisms, such as antibody-dependent cell-mediated cytotoxicity, complement-dependent cytotoxicity, and antibody-dependent cell-mediated phagocytosis.[23,24] Yet, M2e has low immunogenicity and needs to be linked to vaccine carriers to elicit potent antibody responses.[23] Different VLP platforms (e.g., HBc, tobacco mosaic virus, and influenza matrix protein 1 VLPs) and highly immunogenic protein carriers (e.g., flagellin and transcriptional factor GCN4) have been explored to enhance its immunogenicity.[23,24] Studies found that tandem copies of M2e could elicit more potent antibody responses than a single copy of M2e.[23−29] ACAM-FLU-A, the formulation with three copies of M2e linked to the N-terminus of HBc, has been tested in clinical trials with a rapid decline of anti-M2e antibodies.[23] VAX102, the formulation with four

https://doi.org/10.1021/acsami.2c01028
ACS Appl. Mater. Interfaces XXXX, XXX, XXX−XXX

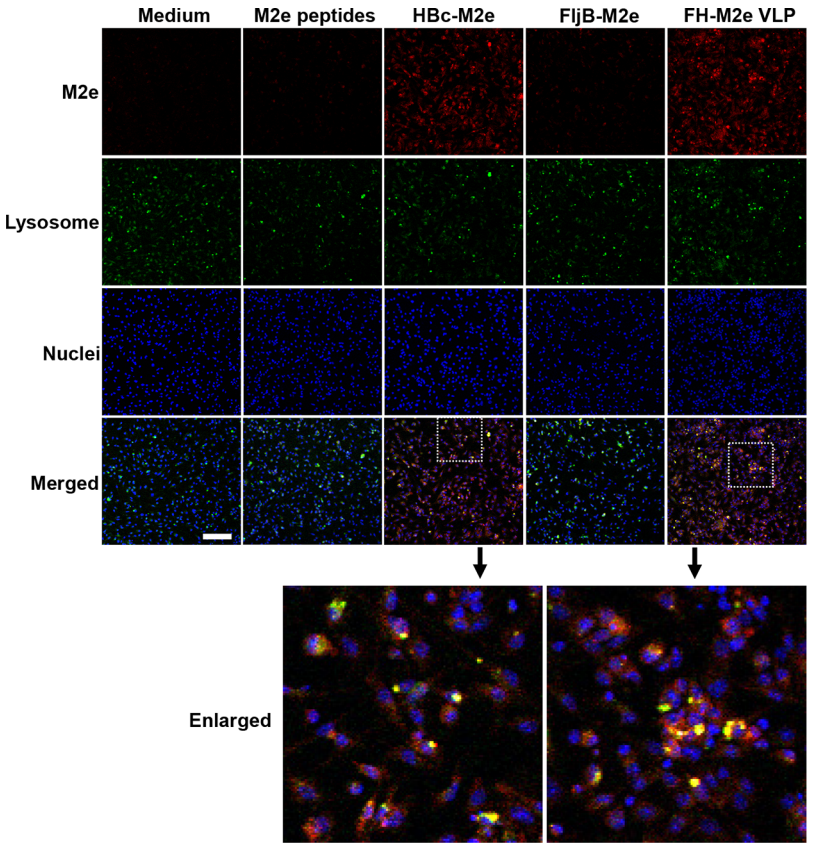

Figure 2. Efficient uptake of FH-M2e VLPs by BMDCs. BMDCs were incubated with M2e peptides, HBc-M2e, FljB-M2e, and FH-M2e VLPs at 70 nM concentration or incubated with medium only in eight-well chamber slides. LysoTracker was added after 1.5 h to stain the acidic organelles. Anti-M2e immune sera (mouse origin) and AF555-labeled goat anti-mouse IgG antibodies were used to stain M2e 3 h after incubation. Cells were counterstained with DAPI and imaged under a fluorescence confocal microscope. Scale: 100 μm. Red: M2e; Green: lysosome; Blue: DAPI. Yellow indicates the overlapping of M2e and lysosome signals.

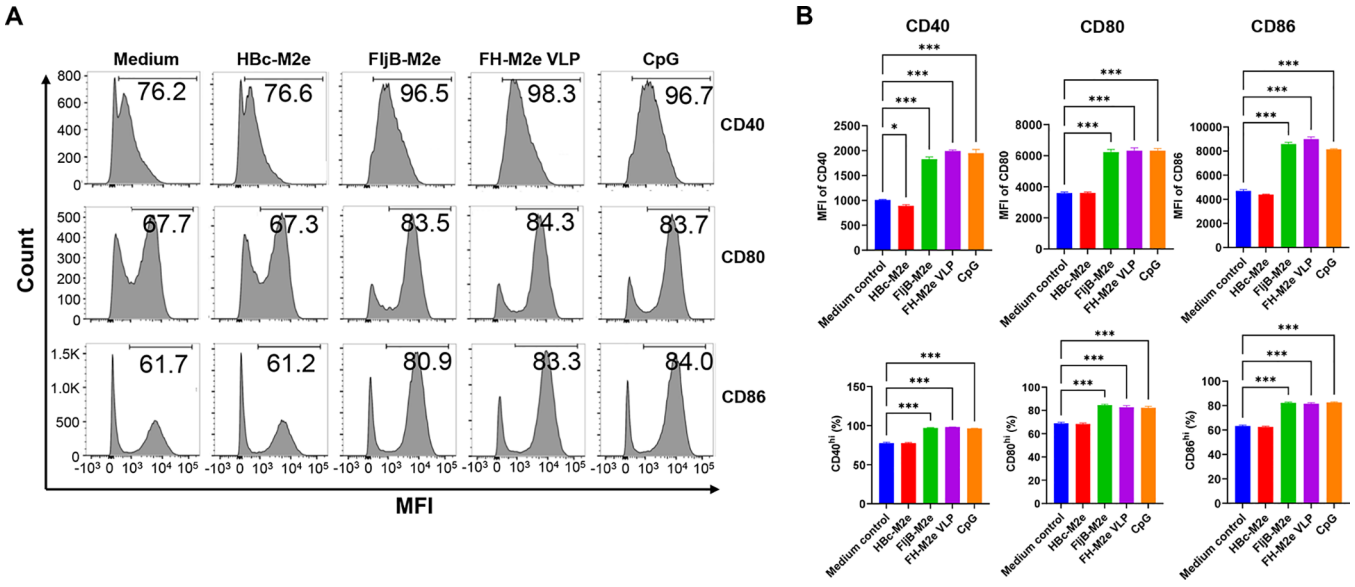

Figure 3. Significant induction of BMDC maturation by FH-M2e VLPs. BMDCs were incubated with M2e peptides, HBc-M2e, FljB-M2e, and FH-M2e VLPs in triplicate at 70 nM concentration or incubated with medium only for 20 h. Cells were then stained with fluorescence-conjugated anti-CD11c, CD40, CD80, and CD86 antibodies, followed by flow cytometry analysis of CD40, CD80, and CD86 expression in $CD11c^+$ cells. (A) Representative histogram of CD40, CD80, and CD86 expression and percentage of $CD40^{hi}$, $CD80^{hi}$, and $CD86^{hi}$ cells in $CD11c^+$ DCs. (B) MFI of CD40, CD80, and CD86 (upper) and percentage of $CD40^{hi}$, $CD80^{hi}$, and $CD86^{hi}$ cells in $CD11c^+$ DCs (lower). One-way ANOVA with Bonferroni's multiple comparison test was used to compare the differences between groups in B. *: $p < 0.05$; ***: $p < 0.001$.

https://doi.org/10.1021/acsami.2c01028
ACS Appl. Mater. Interfaces XXXX, XXX, XXX−XXX

copies of M2e linked to the C-terminus of FljB, was also tested in clinical trials.[19,30] Despite the elicitation of potent anti-M2e antibody responses across a broad dose range (0.3−10 μg), VAX102 stimulated dose-dependent increase of serum C-reactive protein (CRP) levels and a high rate of severe symptoms (43%) in high-dose groups (3 and 10 μg). These studies hint the unmet need of safe and potent vaccine carriers to aid in the development of M2e-based universal influenza vaccines.

This study explored the immunogenicity and safety of our recently developed FH VLP platform for M2e-based vaccine development. Four tandem copies of M2e derived from human H1 and H3, swine H1, and avian H5 and H7 influenza A viruses (Figure S1A), with flexible $(G_4S) \times 2$ linkers inserted between the M2e sequences and also flanking the whole M2e insert, were designed to replace the D3 domain of FljB, followed by *E. coli* expression, purification, and self-assembly to prepare the FH VLP-based M2e vaccine (Figure 1A). The four tandem copies of M2e also replaced the D3 domain of FljB to prepare FljB-M2e or were inserted into the c/e1 loop of HBc to prepare HBc-M2e.

M2e fusion proteins were expressed in *E. coli*, purified, and subjected to SDS-PAGE analysis (Figure 1B). HBc-M2e, FljB-M2e, and FH-M2e fusion proteins showed a higher-than-theoretical molecular weight (MW) (Figures 1B and S1B). The same phenomenon was also observed when different numbers of M2e were inserted into the c/e1 loop of HBc.[27] This could be caused by the high content of acidic amino acids in M2e (20.8−25%, Figure S1A) and the repulsion of negatively charged SDS from binding according to reports.[31,32] The presence of M2e in purified proteins was confirmed by western blotting analysis, with the immune sera collected from mice immunized with keyhole limpet hemocyanin (KLH)-conjugated M2e mixture in the presence of incomplete Freund's adjuvant (Figure 1C). The FH-M2e and HBc-M2e samples were further analyzed by transmission electron microscopy (TEM). VLPs could be readily found in FH-M2e (Figure 1D) but not HBc-M2e samples (data not shown), hinting that the replacement of the D3 domain of FljB by the four tandem copies of M2e did not impair the FH VLP assembly, while the insertion of the four tandem copies of M2e into the c/e1 loop impaired the HBc VLP assembly. Dynamic light scattering (DLS) analysis found that FH-M2e VLPs were about 44 nm in diameter (Figure 1E).

Efficient Uptake and Stimulation of DC Maturation by FH-M2e VLPs. Next, we compared the uptake of different M2e immunogens by bone marrow-derived DCs (BMDCs). As shown in Figure 2, FH-M2e VLPs and HBc-M2e showed a strong uptake, while FljB-M2e and M2e peptides showed a weak uptake by BMDCs. Furthermore, a significant overlap of M2e and lysosomal signals was found in the FH-M2e VLP and HBc-M2e groups (enlarged, Figure 2), hinting that the efficient uptake was through the endolysosomal pathway.

The ability of different M2e immunogens to stimulate BMDC maturation was also explored. As shown in Figure 3A, FH-M2e VLPs and FljB-M2e increased $CD40^{hi}$, $CD80^{hi}$, and $CD86^{hi}$ cells to a level similar to that induced by a clinical CpG 1018 adjuvant (simplified as CpG, hereafter), while HBc-M2e failed to increase the $CD40^{hi}$, $CD80^{hi}$, or $CD86^{hi}$ cell levels. Statistical analysis found that FH-M2e VLPs and FljB-M2e significantly increased the mean fluorescence intensity (MFI) of CD40, CD80, and CD86, similar to or slightly exceeding that stimulated by CpG, while HBc-M2e failed to significantly increase the MFI of CD40, CD80, or CD86 (upper, Figure 3B). Similar trends were found for the percentage of $CD40^{hi}$, $CD80^{hi}$, and $CD86^{hi}$ cells (lower, Figure 3B). These results indicated that FH-M2e VLPs could be efficiently taken up by BMDCs and also stimulate potent BMDC maturation (Table 1). In contrast, HBc-M2e could be efficiently taken up by BMDCs but lacks the ability to stimulate BMDC maturation, while FljB-M2e could stimulate BMDC maturation but lacks efficient uptake by BMDCs (Table 1).

Table 1. Comparison of DC Uptake and Stimulation of DC Maturation

	HBc-M2e	FljB-M2e	FH-M2e VLPs
DC uptake	+++	+	+++
DC maturation	−	+++	+++

FH-M2e VLPs Are More Immunogenic than FljB-M2e and HBc-M2e. The relative immunogenicity of M2e immunogens was then compared by a step-by-step approach. In the first study, we compared FljB-M2e with HBc-M2e and the M2e peptide mixture in the presence of Alum adjuvant (M2e/Alum). As shown in Figure 4A, FljB-M2e induced a significantly higher anti-M2e antibody titer than HBc-M2e and M2e/Alum. As compared to M2e/Alum, HBc-M2e elicited a higher anti-M2e antibody titer, although the difference did not reach a statistically significant level (Figure 4A). FljB-M2e conferred significant protection against body weight loss, following a challenge with 4× LD_{50} of influenza A/Puerto Rico/8/34 H1N1 (PR8) viruses, while HBc-M2e and M2e/Alum failed to confer significant protection (Figure 4B). FljB-M2e conferred 80% protection against lethality, while HBc-M2e and M2e/Alum conferred 25% and 20% protection, respectively (Figure 4C).

In the second study, we compared the relative immunogenicity of FH-M2e VLPs to FljB-M2e, which induced the best protection in the first study. As shown in Figure 4D, FH-M2e VLPs induced significantly higher anti-M2e IgG titer than FljB-M2e. Furthermore, FH-M2e VLPs mainly enhanced anti-M2e IgG2a but not IgG1 titer, which led to a significant increase of anti-M2e IgG2a/IgG1 ratios (Figure 4D). The protective efficacy was then explored by challenging mice with an increased PR8 viral dose (8× LD_{50}) to explore whether FljB-M2e could still induce a good protection. As compared to phosphate-buffered saline (PBS), FH-M2e VLPs significantly reduced the body weight loss, while FljB-M2e failed to significantly reduce the body weight loss (Figure 4E). FH-M2e VLPs conferred 60% protection against lethality, while FljB-M2e failed to confer any protection at the increased viral challenge dose (Figure 4E). To explore whether FH-M2e VLPs could elicit superior protection against other influenza A viral strains, another round of immunization and challenge studies was conducted. FH-M2e VLPs were found to induce a significantly higher anti-M2e antibody titer than FljB-M2e (Figure S3). The mice were then randomly divided into two groups and challenged with mouse-adapted influenza pandemic 2009 H1N1 (A/California/07/2009, pdm09) or influenza A/Philippines/2/82 H3N2 viruses. As shown in Figure 4F, FH-M2e VLPs significantly reduced the body weight loss after pdm09 viral challenges, while FljB-M2e failed to reduce the body weight loss. FH-M2e VLPs conferred 75% protection against lethality induced by pdm09 viruses, while FljB-M2e failed to confer any protection (Figure 4F). After

https://doi.org/10.1021/acsami.2c01028
ACS Appl. Mater. Interfaces XXXX, XXX, XXX−XXX

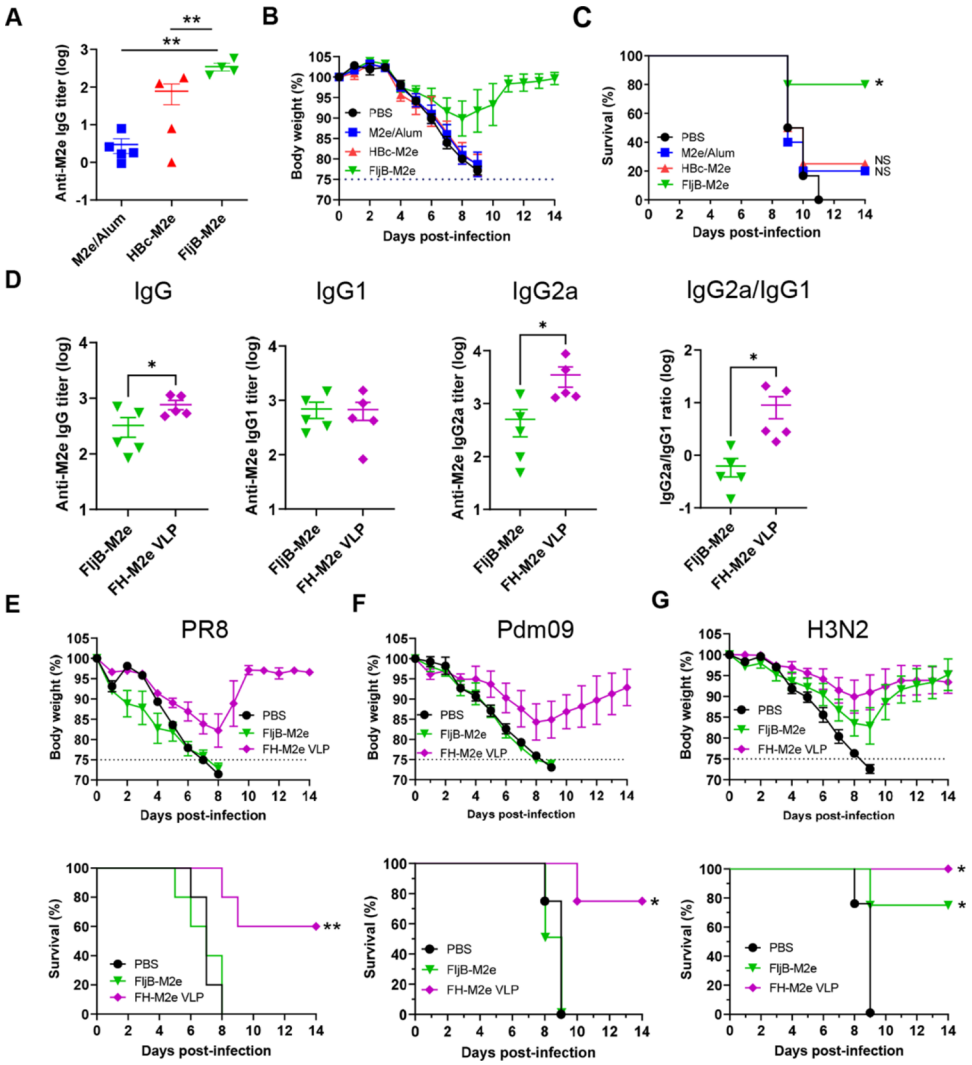

Figure 4. Superior immunogenicity and protective efficacy of FH-M2e VLPs. (A−C) BALB/c mice were intramuscularly immunized with 5 μg FljB-m2e, 2.7 μg HBc-M2e that contained an equal amount of M2e, or a mixture of four different M2e peptides (10 μg each) in the presence of Alum adjuvant (Alhydrogel) or immunized with PBS as a negative control. Immunization was repeated after 3 weeks. Serum anti-M2e antibody titer was measured 3 weeks after boost and shown in A. Mice were then intranasally challenged with 4× LD_{50} of PR8 viruses 4 weeks after boost. Body weight (B) and survival (C) were monitored daily for 14 days. (D) BALB/c mice were intramuscularly immunized with 6.5 μg FH-M2e VLPs or 5 μg FljB-M2e that contained the same amount of M2e or immunized with PBS as a negative control. Immunization was repeated after 3 weeks. Serum anti-M2e IgG and the subtype IgG1 and IgG2a antibody titers were measured 3 weeks after boost. The ratio of IgG2a/IgG1 antibody titers was also calculated. (E) Mice were then challenged with 8× LD_{50} of PR8 viruses 4 weeks after boost. Body weight loss (upper) and survival (lower) were monitored daily for 14 days. (F,G) BALB/c mice were similarly immunized as in D and then randomly divided into two groups for challenge with 2× LD_{50} of pdm09 (F) or 5× LD_{50} of influenza A/Philippines/2/82 H3N2 viruses (G). Body weight (upper) and survival (lower) were similarly monitored as in E. n = 4−5 in A−C; n = 5 in D−E; n = 4 in F−G. One-way ANOVA with Tukey's multiple comparison test was used to compare the differences among groups in A. Two-tailed Student's t test was used to compare the differences in D. Log-rank test with Bonferroni's correction was used to compare the differences of survival between the vaccine and PBS groups in C and lower panels of E−G. *, $p < 0.05$; **, $p < 0.01$. NS: not significant.

H3N2 viral challenges, the FH-M2e VLP group showed a slower rate of body weight loss as compared to the FljB-M2e group (Figure 4G). FH-M2e VLPs conferred 100% protection against H3N2 viral challenges, while FljB-M2e conferred only 75% protection (Figure 4G).

It was reported that flagellin-based vaccines elicited systemic adverse reactions in humans.[18−21] In the above first and second studies, we monitored the serum proinflammatory cytokine levels 3 and 18 h after immunization to gain insights on the potential of various M2e immunogens to induce systemic adverse reactions.[33] As shown in Figure 5, FljB-M2e immunization in both studies significantly increased serum IL-6 and TNFα levels 3 h after prime and boost immunizations, while HBc-M2e and M2e peptide immunizations in the first study and FH-M2e VLP immunization in the second study did not significantly increase serum IL-6 or TNFα levels. These results were in line with prior reports that flagellin-based influenza vaccines carry the risk of inducing systemic adverse reactions.[18−21] Our data support a good systemic safety of FH-M2e VLPs. Besides the systemic cytokine release, we also monitored the rectal temperature before and 24 h after immunization in the above studies. We failed to detect a significant increase of rectal temperature in any group (data not shown). To explore whether the rectal

https://doi.org/10.1021/acsami.2c01028
ACS Appl. Mater. Interfaces XXXX, XXX, XXX−XXX

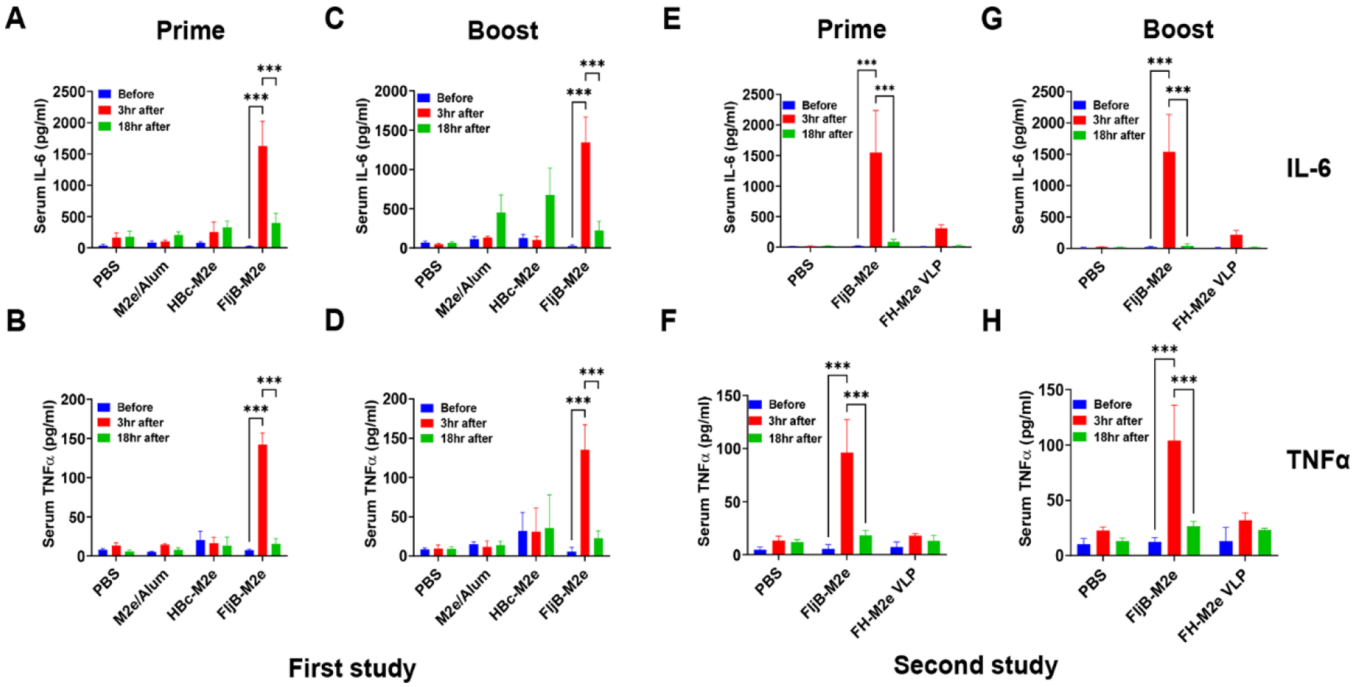

Figure 5. Systemic cytokine release induced by FljB-M2e but not FH-M2e VLPs. (A–D) Serum IL-6 (A,C) and TNFα levels (B,D) of mice in the first study (Figure 4A–C) were measured before immunization and 3 and 18 h after prime and boost immunizations. (E–H) Serum IL-6 (E,G) and TNFα levels (F,H) of mice in the second study (Figure 4D,E) were measured before immunization and 3 and 18 h after primer and boost immunizations. n = 4–5 in A–D and n = 5 in E–H. Two-way ANOVA with Tukey's multiple comparison test was used to compare the cytokine level differences at different time points within the group. ***, $p < 0.001$.

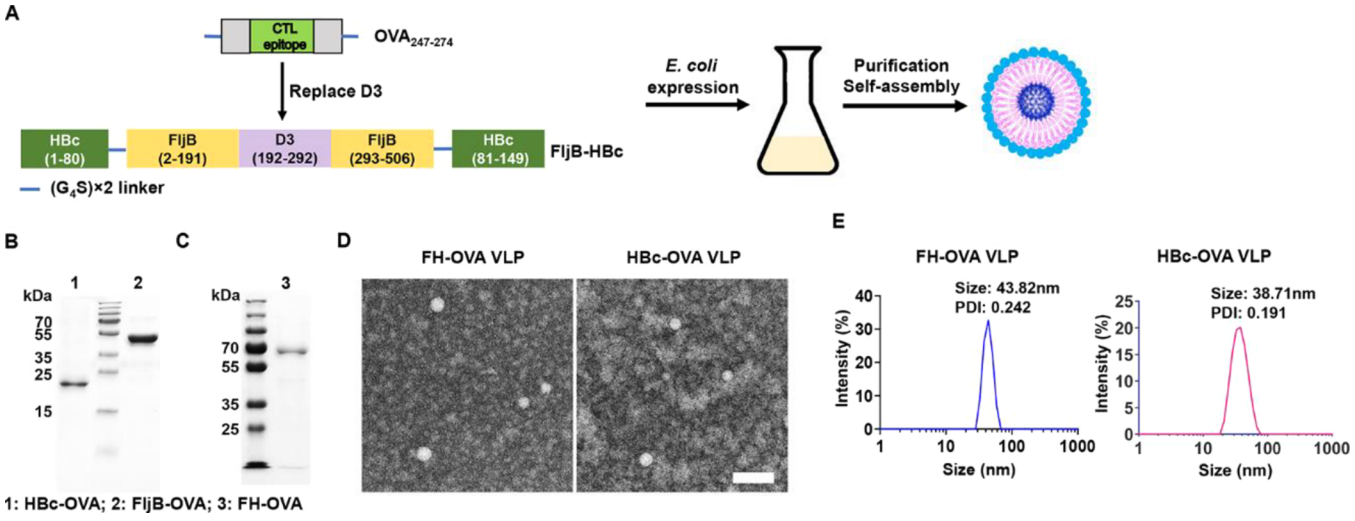

Figure 6. FH-OVA VLP vaccine design and characterization. (A) Schematic illustration of the FH-OVA VLP vaccine design and preparation. CTL epitope (SIINFEKL) was located in the center of $OVA_{247-274}$. (B) Purified HBc-OVA and FljB-OVA were subjected to SDS-PAGE analysis. (C) Purified FH-OVA was subjected to SDS-PAGE analysis. (D) TEM analysis of FH-OVA and HBc-OVA samples. Scale: 100 nm. (E) DLS analysis of FH-OVA and HBc-OVA VLPs in Zetasizer Nano ZS (Malvern).

temperature increase could be observed at higher vaccine doses, the mice were intradermally injected with 25 μg FljB-M2e or 32.5 μg FH-M2e VLPs (equal M2e amount, with fivefold increase of dose). We found that 25 μg FljB-M2e significantly increased the rectal temperature of mice, while 32.5 μg FH-M2e VLPs failed to increase the rectal temperature of mice (Figure S3). Furthermore, FH-M2e VLPs at the increased dose did not significantly increase serum IL-6 or TNFα levels (Figure S4). Overall, these studies support a good systemic safety of FH-M2e VLPs across a broad dose range.

FH-OVA VLPs Are More Immunogenic than HBc-OVA VLPs and FljB-OVA. The above studies support the high potency of FH VLPs as a vaccine platform to elicit potent humoral immune responses against surface-displayed vaccine antigens. Next, we explored the potency of FH VLPs to elicit CTL responses against surface-displayed vaccine antigens. To this end, the $OVA_{247-274}$ peptide comprising the CTL epitope of OVA (SIINFEKL) in the center (Figure S5A) was designed to replace the D3 domain of FljB for display on the FH VLP surface, as illustrated in Figure 6A. The same peptide also

https://doi.org/10.1021/acsami.2c01028
ACS Appl. Mater. Interfaces XXXX, XXX, XXX–XXX

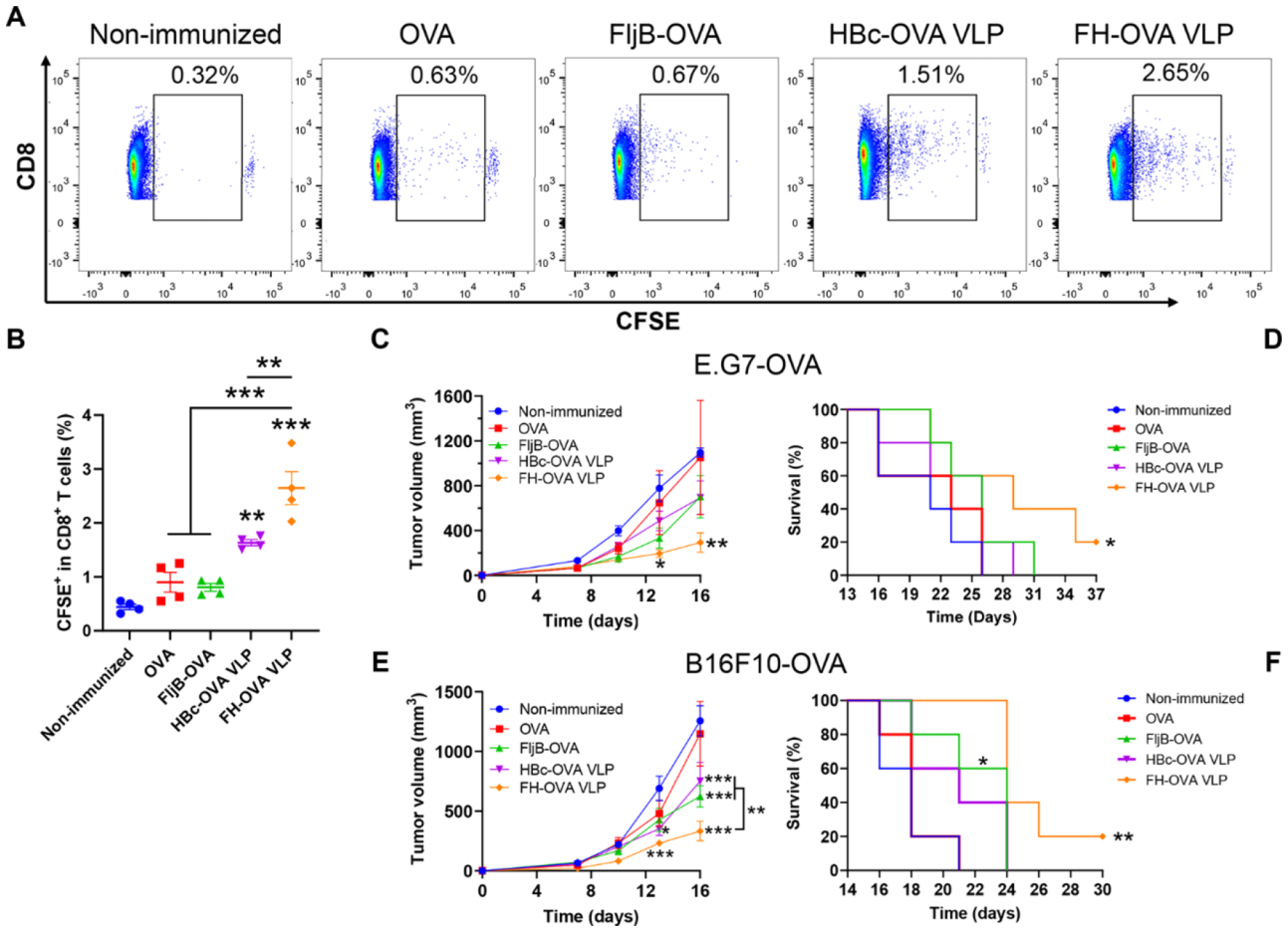

Figure 7. Superior immunogenicity and protective efficacy of FH-OVA VLPs. (A,B) OT-I T cells were purified, stained with CFSE, and intravenously injected into C57BL/6 mice. The mice were then intradermally immunized with FH-OVA VLPs, HBc-OVA VLPs, FljB-OVA, and OVA peptide that contained the same amount of OVA portion, or left non-immunized as a negative control. Draining LNs were collected after 4 days. Single cells were prepared, stained with fluorescence-conjugated anti-CD4 and CD8 antibodies, and analyzed by flow cytometry. Cells were first gated based on FSC and SSC and then based on CD4 and CD8 expression. $CFSE^+$ cells (exclusion of cells with the maximal CFSE signals that represented the adoptive transferred nondividing OT-I T cells) were then gated from $CD8^+$ ($CD4^-$) cell populations. Representative dot plots of dividing $CFSE^+$ cells in $CD8^+$ T cells are shown in **A**. Statistical analysis of percentage of $CFSE^+$ cells in $CD8^+$ T cells is shown in B. (C,D) C57BL/6 mice were intradermally immunized with FH-OVA VLPs, HBc-OVA VLPs, FljB-OVA, and OVA peptide that contained the same amount of OVA portion or left non-immunized as a negative control. Immunization was repeated two more times at 3-week intervals. Mice were then subcutaneously challenged with E.G7-OVA lymphoma cells 2 weeks after the last immunization. Tumor growth was monitored and shown in C. Survival of tumor-bearing mice is shown in D. (E,F) C57BL/6 mice were similarly immunized as in C-D, followed by the subcutaneous challenge of B16F10-OVA melanoma cells 2 weeks after the last immunization. Tumor growth is shown in E. Survival of tumor-bearing mice is shown in F. n = 4 in A–B; n = 5 in C–D and E–F. One-way ANOVA with Tukey's multiple comparison test was used to compare the differences among groups in A. Two-way ANOVA with Tukey's multiple comparison test was used to compare tumor volume differences at different time points between groups in C and E. Log-rank test with Bonferroni's correction was used to compare the differences of survival between groups in D and F. *, $p < 0.05$; **, $p < 0.01$; ***, $p < 0.001$.

replaced the D3 domain of FljB or was inserted into the c/e1 loop of HBc to prepare FljB- or HBc-based OVA peptide vaccine. OVA peptide-fusion proteins were analyzed by SDS-PAGE (Figure 6B,C), and the estimated molecular weights matched well with the theoretical ones (Figure S5B). After refolding, both FH-OVA and HBc-OVA formed VLPs (Figure 6D) with an average diameter of ~44 and 39 nm, respectively (Figure 6E).

The relative potency of FH-OVA VLPs to induce OVA-specific CTL responses was then compared with HBc-OVA VLPs, FljB-OVA, and the synthesized $OVA_{247-274}$ peptide (short as OVA). Due to the low abundance of OVA-specific $CD8^+$ T cells in physiological conditions, we adoptively transferred OVA-specific $CD8^+$ T cells from OT-I mice to C57BL/6 mice, followed by intradermal immunization of the diverse OVA immunogens. Draining lymph nodes (LNs) were harvested after 4 days, and the percentage of $CFSE^+$ cells in $CD8^+$ T cells was analyzed. As shown in Figure 7A, FH-OVA VLPs induced the most significant expansion of adoptively transferred OT-I T cells, followed by HBc VLPs and then FljB-OVA and OVA peptide. Statistical analysis indicated that FH-OVA VLPs were more potent than HBc-OVA VLPs or FljB-OVA to stimulate OT-I T cell expansion (Figure 7B).

Next, the mice were intradermally immunized with the different OVA immunogens that contained an equal OVA content. Immunization was repeated two more times. Cellular immune responses in peripheral blood mononuclear cells (PBMCs) were analyzed 7 days after the last immunization. As shown in Figure S6A,B, FH-OVA VLPs significantly increased IFNγ and IL4-secreting $CD8^+$ T cells, while HBc-OVA VLPs

https://doi.org/10.1021/acsami.2c01028
ACS Appl. Mater. Interfaces XXXX, XXX, XXX–XXX

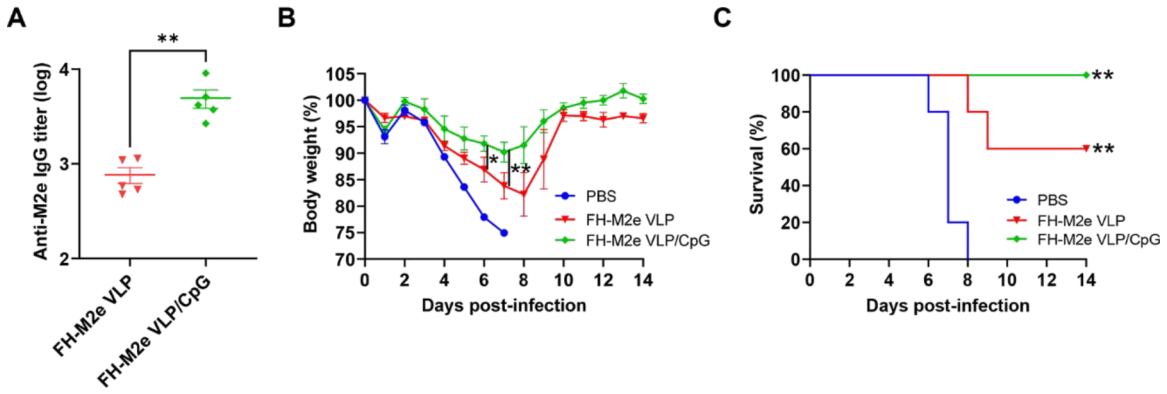

Figure 8. CpG 1018 boosts FH-M2e VLP immunization. BALB/c mice were intramuscularly immunized with 24.3 μg FH-M2e VLPs alone or in the presence of 2 μg CpG 1018 or immunized with PBS as a negative control. The immunization was repeated after 3 weeks. Serum anti-M2e antibody titer was measured 3 weeks after boost and shown in A. Mice were intranasally challenged with 8× LD_{50} of PR8 viruses 4 weeks after boost. Body weight (B) and survival (C) were monitored daily for 14 days. n = 5. One-way ANOVA with Tukey's multiple comparison test was used to compare the differences between the groups in A. Two-way ANOVA with Tukey's multiple comparison test was used to compare the differences of body weight loss on individual days between groups in B. Log-rank test with Bonferroni's correction was used to compare the differences of survival between the vaccine and PBS groups in C. *, $p < 0.05$; **, $p < 0.01$.

significantly increased IFNγ but not IL4-secreting $CD8^+$ T cells. Interestingly, FH-OVA VLPs also significantly increased IFNγ and IL4-secreting $CD4^+$ T cells, while other immunogens failed to do so (Figure S6C,D). Antitumor immunity was then explored by challenging mice with OVA-expressing E.G7 lymphoma. FH-OVA VLP immunization most significantly retarded E.G7-OVA lymphoma growth, with the tumor volume significantly smaller than that in the non-immunized group on days 13 and 16 (Figure 7C). In contrast, HBc-OVA VLP, FljB-OVA, and OVA peptide immunization failed to significantly inhibit the E.G7-OVA lymphoma growth (Figure 7C). FH-OVA VLP immunization also significantly extended the survival of E.G7-OVA tumor-bearing mice, while the other immunizations failed to do so (Figure 7D). To explore whether FH-OVA VLP-elicited protection is tumor-specific, the mice were similarly immunized but challenged with OVA-expressing B16F10 melanoma. As shown in Figure 7E, FH-OVA VLP immunization most significantly retarded B16F10-OVA melanoma growth as compared to HBc-OVA or FljB-OVA immunization, while the latter two also significantly retarded B16F10-OVA melanoma growth as compared to the non-immunized negative control. Tumor volume was significantly smaller on days 13 and 16 in the FH-OVA VLP group than that in the non-immunized group. Tumor volume was also significantly smaller on day 16 in the FH-OVA VLP group than that in the HBc-OVA or FljB-OVA group. FH-OVA VLP immunization significantly extended the survival of B16F10-OVA tumor-bearing mice, while HBc-OVA VLP immunization failed to do so (Figure 7F). FljB-OVA also significantly extended the survival of B16F10-OVA tumor-bearing mice though to a lesser extent than FH-OVA VLPs (Figure 7F). These data indicated that FH VLPs were more immunogenic than HBc VLPs and FljB for the OVA peptide display to elicit CTL responses and antitumor immunity.

Although we mainly focused on the evaluation of CTL responses, we also measured the serum anti-$OVA_{247-274}$ antibody titer after the last immunization. As shown in Figure S7A, FljB-OVA and FH-OVA VLPs but not HBc-OVA VLPs induced a significantly higher anti-OVA IgG titer than OVA immunization alone. Furthermore, FljB-OVA induced a significantly higher IgG1 titer, while FH-OVA VLP induced a significantly higher IgG2c titer (Figure S7B,C). These data indicated that FH-OVA VLPs induced Th1-biased antibody responses, while FljB-OVA induced Th2-biased antibody responses, in line with our previous report.[22]

Systemic safety was also evaluated in the above studies. As shown in Figure S8, FljB-OVA induced the most significant increase of serum IL-6 and TNFα levels 3 h after each immunization, while FH-OVA VLPs did not significantly increase serum IL-6 or TNFα levels. Interestingly, repeated FljB-OVA immunizations induced gradually reducing serum IL-6 and TNFα levels at 3 h (Figure S8), which was not observed after repeated FljB-M2e immunizations (Figure 5A–D), hinting that this phenomenon might be antigen-specific. Considering the overt activation of TLR5 might be the cause of systemic adverse reactions associated with FljB-based vaccines, we compared the TLR5 activation ability of D3 domain-deleted FH VLPs ($FH_{\Delta D3}$ VLP), FH VLPs (D3 domain intact), FH-OVA VLPs, FljB, and FljB-OVA in a commercially available TLR5 reporter assay. As shown in Figure S9, FljB-OVA activated TLR5 similar to that of native FljB, indicating that the replacement of the D3 domain with OVA peptide did not impact the TLR5 activation ability. FH-OVA VLPs showed much weakened TLR5 activation as compared to FljB-OVA and similar TLR5 activation to $FH_{\Delta D3}$ VLPs (Figure S9). Interestingly, $FH_{\Delta D3}$ VLPs showed increased TLR5 activation as compared to FH VLPs (Figure S9), which might be due to the increased accessibility of the D1 domain (responsible for TLR5 activation) to TLR5 after the removal of D3 domain.

CpG 1018 Boosts FH-M2e VLP and FH-OVA VLP Immunization. The above studies identified high immunogenicity of FH VLP-based vaccines in the absence of additional adjuvants. Our previous studies found that CpG adjuvant could efficiently boost FH VLP-based nicotine vaccination.[22] Here, we explored whether the incorporation of a clinical CpG 1018 adjuvant, which is broadly effective in mice, nonhuman primates, and humans,[34,35] could further enhance FH-M2e VLP and FH-OVA VLP vaccine efficacy. A low dose of CpG 1018 (2 μg) was explored to boost FH-M2e VLP immunization. As shown in Figure 8A, CpG 1018 significantly increased the FH-M2e VLP-induced anti-M2e antibody titer

https://doi.org/10.1021/acsami.2c01028
ACS Appl. Mater. Interfaces XXXX, XXX, XXX−XXX

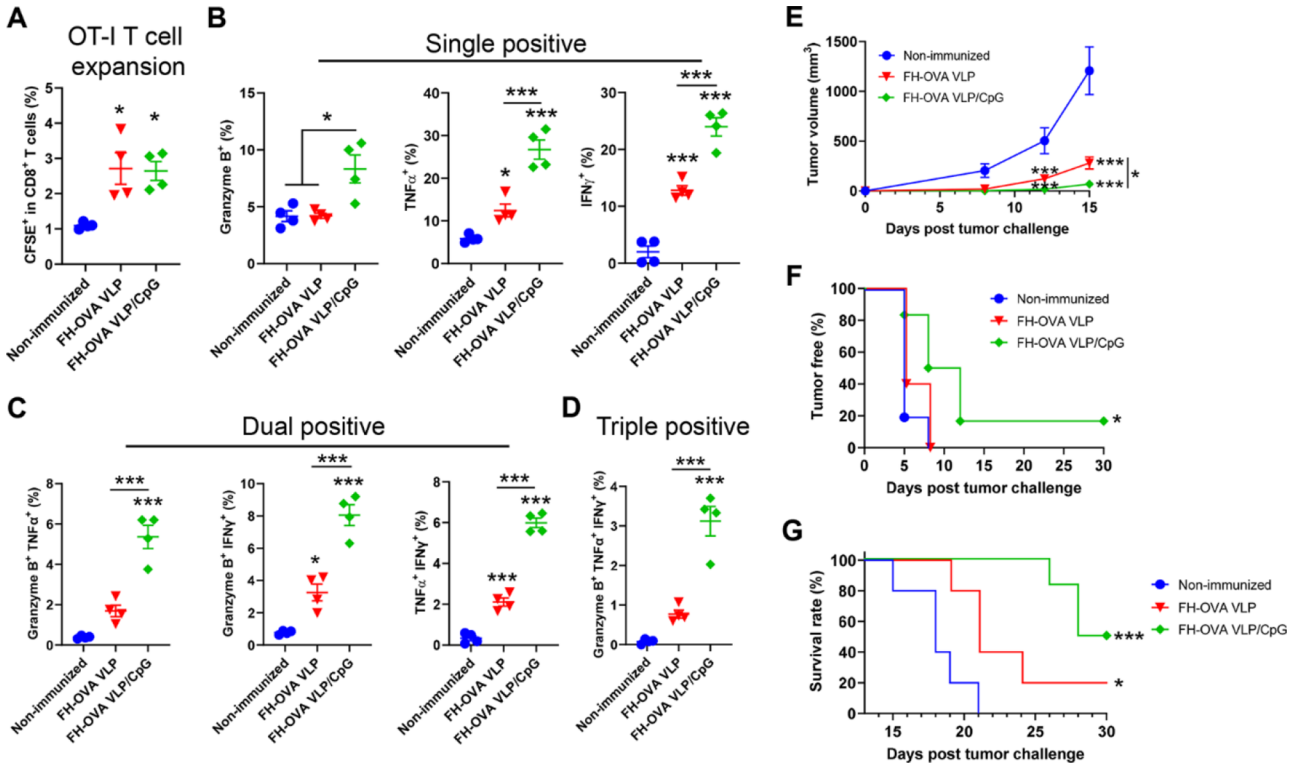

Figure 9. CpG 1018 boosts FH-OVA VLP immunization. (A) OT-I T cells were adoptively transferred to C57BL/6 mice. Mice were intradermally immunized with 8 μg FH-OVA VLPs in the presence or absence of 40 μg CpG 1018 after 24 h or left non-immunized as a negative control. Draining LNs were collected after 4 days, stimulated with the CTL epitope of OVA in the presence of anti-CD28 antibodies overnight. Brefeldin A was added, and after 5 h, cells were harvested and stained with fluorescence-conjugated antibodies. The percentage of $CFSE^+$ cells in $CD8^+$ T cells (A) and single (B), dual (C), and triple cytokine-secreting cells (D) in $CFSE^+$ $CD8^+$ T cells were compared between groups. (E–G) Mice were subjected to FH-OVA VLP immunization in the presence or absence of CpG 1018 or left non-immunized as a negative control. Immunization was repeated three times at 3-week intervals. The mice were then subcutaneously challenged with B16F10-OVA melanoma 2 weeks after the last immunization. Tumor growth and survival were monitored for 30 days. Tumor growth, tumor-free rate, and survival of tumor-bearing mice are shown in E–G, respectively. $n = 4$ in A–D. $n = 5$–6 in E–G. One-way ANOVA with Tukey's multiple comparison test was used to compare the differences between groups in A–D. Two-way ANOVA with Tukey's multiple comparison test was used to compare the tumor volume differences at different time points between groups in E. Log-rank test with Bonferroni's correction was used to compare the differences of survival between groups in F,G. *, $p < 0.05$; ***, $p < 0.001$.

by 6.5-fold. After PR8 viral challenges (8× LD_{50}), FH-M2e VLPs with CpG 1018 adjuvant conferred better protection than FH-M2e VLP alone (Figure 8B,C). Significantly less body weight loss was observed in the FH-M2e VLP/CpG group on days 6 and 7 than that in the FH-M2e VLP group (Figure 8B). FH-M2e VLPs with CpG 1018 adjuvant conferred 100% protection against lethality, while FH-M2e VLPs only conferred 60% protection (Figure 8C).

Next, 40 μg CpG 1018 was explored to boost FH-OVA VLP immunization as our pilot studies found that a low dose of 2 μg CpG 1018 was ineffective to boost FH-OVA VLP immunization. We first explored the ability of the CpG 1018 adjuvant to enhance FH-OVA VLP-induced OT-I T cell expansion and the ability of expanded OT-I T cells to secrete Granzyme B, TNFα, and IFNγ, with crucial roles in antitumor immunity. As shown in Figure 9A, the incorporation of CpG did not further enhance OT-I T cell expansion. However, CpG 1018 significantly increased single (Figure 9B), dual (Figure 9C), and triple cytokine-secreting OT-I T cells (Figure 9D). The mice were then immunized with FH-OVA VLPs in the presence or absence of CpG 1018 or left non-immunized as a negative control. Immunization was repeated two more times and 1 week after the last immunization, PBMCs were collected, stimulated with CTL epitope of OVA, and cytokine-secreting OVA-specific $CD8^+$ T cells were analyzed by tetramer staining and flow cytometry analysis. As shown in Figure S10, incorporation of CpG 1018 into FH-OVA VLP immunization significantly enhanced OVA-specific single, dual, and triple cytokine-secreting $CD8^+$ T cells, confirming the results of adoptive transfer studies. We further found that CpG 1018 adjuvant increased anti-OVA IgG and subtype IgG2c but not IgG1 antibody titer (Figure S11A–C). The ratio of IgG2c to IgG1 was significantly increased by the incorporation of CpG 1018 adjuvant (Figure S11D), hinting the potentiation of Th1-biased antibody responses.

Regarding systemic safety, we found that FH-OVA VLP immunization in the presence of 40 μg CpG 1018 significantly increased serum IL-6 and TNFα levels at 3 h (Figure S12). The maximal cytokine release occurred after the first immunization, as observed in FljB-OVA immunization (Figure S8). Yet, the maximal IL-6 levels induced by FH-OVA VLPs in the presence of CpG 1018 were only 18% of that induced by FljB-OVA (Figures S8A and S12A). Interestingly, FH-OVA VLP immunization in the presence of CpG 1018 induced 61% higher serum TNFα levels than FljB-OVA (Figures S8B and S12B). These results indicated the induction of a mild systemic cytokine release after the incorporation of CpG 1018 into FH-OVA VLP immunization.

https://doi.org/10.1021/acsami.2c01028
ACS Appl. Mater. Interfaces XXXX, XXX, XXX–XXX

The mice were then challenged with B16F10-OVA melanoma. As shown in Figure 9E, FH-OVA VLP immunization alone significantly retarded tumor growth, and the incorporation of CpG 1018 further retarded tumor growth. Interestingly, FH-OVA VLP immunization in the presence of CpG 1018 prevented tumor growth in 16.7% of mice (Figure 9F). FH-OVA VLP immunization significantly extended the survival of tumor-bearing mice, while the incorporation of CpG 1018 into FH-OVA VLP immunization more significantly extended the survival of tumor-bearing mice (Figure 9G). These results indicated that CpG 1018 was highly potent to further enhance FH-OVA VLP-induced CTL responses and antitumor immunity.

DISCUSSION

This study proved FH VLPs to be a highly immunogenic, safe, and versatile platform for vaccine development to elicit potent humoral and cellular immune responses. FH VLPs showed higher immunogenicity for M2e-based universal influenza vaccine development and OVA-based tumor vaccine development as compared to FljB and HBc VLPs. FH-M2e VLPs elicited the highest anti-M2e antibody titer among the three, while FljB-M2e elicited a higher anti-M2e antibody titer than HBc-M2e. FH-M2e VLPs conferred superior protection against multiple influenza A viral strains, while FljB-M2e failed to elicit significant protection or elicited much weaker protection. These data support FH-M2e VLPs to be a good universal influenza vaccine candidate capable of eliciting potent cross-protective anti-M2e antibody responses. For OVA-based tumor vaccine development, FH-OVA VLPs stimulated the most potent anti-OVA CTL responses and most significantly suppress OVA-expressing tumor growth when compared to FljB-OVA or HBc-OVA VLPs, while the latter two elicited similar antitumor immunity. Although FH VLP-based vaccines alone were highly immunogenic, we found that the incorporation of CpG 1018 adjuvant could further enhance their immunogenicity. Interestingly, a low dose of CpG 1018 (2 μg) was highly effective to enhance FH-M2e VLP-induced anti-M2e antibody responses while ineffective to potentiate FH-OVA VLP-induced antitumor immunity (data not shown). Instead, 40 μg CpG 1018 was found to significantly enhance FH-OVA VLP-induced antitumor immunity. The requirement of diverse CpG 1018 amounts to potentiate anti-M2e antibody responses and anti-OVA CTL responses remains to be explored but may reflect the differential needs of diverse CpG 1018 amounts to potentiate FH VLP vaccine-induced humoral and cellular immune responses.

The high immunogenicity of FH VLP-based vaccines is believed to be due to their efficient uptake by DCs and also induction of strong DC maturation. Despite their efficient uptake, VLPs often lack the ability to stimulate strong DC maturation. The ability of FH-VLPs and FH-M2e VLPs to induce DC maturation is expected to be contributed by surface-displayed FljB, considering that HBc VLPs in our prior study or HBc-M2e failed to induce DC maturation (Figure 3).[22] Our studies further found that DC maturation did not require a strong activation of TLR5 due to the weak TLR5 activation by FH VLPs or FH-OVA VLPs (Figure S9).[22] The significantly reduced TLR5 activation was most likely due to the high-density display of FljB on the HBc VLP surface, which embedded the D1 domain of FljB, responsible for TLR5 activation, in the interior of FH VLPs. In support, removal of the D3 domain of FljB partially increased TLR5 activation ability ($FH_{\Delta D3}$ VLP vs FH VLP, Figure S9), while the surface display of a short OVA peptide slightly reduced the TLR5 activation ability (highest concentration, FH-OVA VLP vs $FH_{\Delta D3}$ VLP, Figure S9).

FH-M2e VLPs elicited Th1-biased antibody responses, while FljB-M2e elicited Th2-biased antibody responses. Although the OVA peptide used in our study mainly contained CTL epitope, FH-OVA VLPs were found to elicit Th1-biased antibody responses, and FljB-OVA was found to elicit Th2-biased antibody responses. These results were in line with our previous finding that FH VLPs mainly induced Th1-biased antibody responses, while FljB mainly induced Th2-biased antibody responses.[22] The ability of FH VLPs, FljB, and their respective vaccines to induce differential Th1- and Th2-biased antibody responses may reflect their differential stimulation of diverse DC, T, and B cell responses. Th1-biased immune responses were in line with the ability of FH-OVA VLPs to stimulate potent CTL responses.[36] Our studies found that the incorporation of CpG 1018, a Th1-biased adjuvant,[34] could further enhance FH-OVA VLP-induced Th1-biased antibody responses and CTL responses. These results hinted the potential synergy between FH VLP surface-displayed FljB and CpG 1018 in the induction of CTL responses and antitumor immunity.

Our studies found that the four tandem copies of M2e and the CTL epitope of OVA (146 and 48 aa, respectively, with the linker included) could be readily displayed on the FH VLP surface via D3 domain replacement. In contrast, insertion of four tandem copies of M2e into the c/e1 loop of HBc impacted VLP assembly. The inability of M2e-inserted HBc to assemble into VLPs contradicted with a prior study, in which the four tandem copies of M2e were also inserted into the c/e1 loop of HBc without affecting the VLP assembly.[27] Such a discrepancy could be caused by the different linker and M2e designs. A much longer linker (19 aa) was used in the prior report, and the linker was not inserted between M2e sequences.[27] M2e in our study ended with an additional proline (P), which was known to change the direction of polypeptide chains.[37] Furthermore, the tandem copies of M2e were inserted between D78 and S81 in the prior study,[27] while the tandem copies of M2e were inserted between A80 and S81 in our study. HBc used in the prior study lacked the first three amino acids and contained an additional cysteine at the end of the truncated sequence.[27] Two enzymatic digestion sites were also inserted between D78 and S81 in the prior study.[27] All these might contribute to the different outcomes of HBc-M2e folding, while the major factor(s) that affected the HBc-M2e VLP assembly in our study remained to be explored. Considering that long antigenic peptides between 200 and 400 aa successfully replaced the D3 domain of flagellin to generate flagellin-based vaccines without affecting the TLR5 activation ability,[15−17] we believe that longer antigenic epitopes can also be displayed on the FH VLP surface via D3 domain replacement. Thus, FH VLPs may serve as a highly versatile platform for the display of long antigenic epitopes or even full-length protein antigens.

FH VLP-based vaccines also showed a good systemic safety without the induction of systemic IL-6 or TNFα release. Systemic adverse reactions have been linked to flagellin-based vaccines.[18−20,38] Clinical adverse reactions include a significant increase of serum CRP levels, significant increase of serum IL-6 levels, and increase of body temperature in some participants.[18−20,38] Also, the systemic adverse reactions were

https://doi.org/10.1021/acsami.2c01028
ACS Appl. Mater. Interfaces XXXX, XXX, XXX−XXX

vaccine dose-dependent, with higher doses associated with more frequent and severe adverse reactions.[18−20,38] Despite the good immunogenicity of flagellin-based vaccines in clinical trials, the high risk to cause systemic adverse reactions discouraged their further development. The systemic adverse reactions observed in flagellin-based vaccines were expected to be mediated by the overt activation of TLR5, considering TLR5 activation leads to IL-6 synthesis, which further activates CRP release.[39,40] A significantly reduced TLR5 activation explained the significantly improved systemic safety of FH VLP-based vaccines in our studies. Interestingly, the significant reduction of TLR5 activation did not affect the DC activation and immunogenicity of FH VLP-based vaccines.

CONCLUSIONS

HBc VLPs and flagellin are highly immunogenic vaccine delivery platforms and have been extensively explored for vaccine development against bacterial, viral, and parasitic diseases and cancer.[6,12] Despite many years of research, there are no HBc VLP- or flagellin-based vaccines approved for human use yet. Our study presents a hybrid flagellin/HBc VLP platform (FH VLPs) that is potentially more immunogenic, safer, and more versatile than the parent platforms to support vaccine development to elicit potent humoral and cellular immune responses.

MATERIALS AND METHODS

Reagents. All enzymes used in molecular cloning experiments were purchased from New England Biolabs (Ipswich, MA). Isopropyl-β-D-thiogalactoside (IPTG, R0393) and Ni-NTA Agarose (R90115) were purchased from Thermo Fisher Scientific (Waltham, MA). Fluorescence-conjugated antibodies used in immunostaining and flow cytometry were purchased from Biolegend (San Diego, CA) or Thermo Fisher Scientific (Waltham, MA). LysoTracker Deep Red (L12492), eight-well chamber slides (Nunc Lab-Tek Chamber Slide, 177442), and protease and phosphatase inhibitor cocktail (78442) were purchased from Thermo Fisher Scientific (Waltham, MA). Endotoxin-free OVA, Alum adjuvant (Alhydrogel, 2%), and HEK-Blue mTLR5 cell line (hkb-mtlr5) were purchased from Invivogen (San Diego, CA). CpG 1018 was synthesized by Trilink Biotechnologies (San Diego, CA). AF555 goat antimouse IgG (ab150114) and antifade fluorescence mounting medium with DAPI (ab104139) were purchased from Abcam (Cambridge, MA).

Animals. Male BALB/c and female C57BL/6 mice (6−8 weeks old) were purchased from Charles River Laboratories (Wilmington, MA). OT-I transgenic mice (003831) were obtained from Jackson Laboratory (Bar Harbor, ME). The animals were housed in the animal facilities of University of Rhode Island. The mice were anesthetized by intraperitoneal injection of ketamine (80 mg/kg) and xylazine (10 mg/kg) for hair removal and immunization. Animal experiments involving influenza viruses were conducted in the animal biosafety level 2 facility of University of Rhode Island. All animal procedures were approved by the Institutional Animal Care and Use Committee of University of Rhode Island.

Recombinant Plasmid Construction. Four tandem copies of M2e from human H1 and H3, swine H1N1, and avian H5N1 and H7N9 were chosen to construct recombinant plasmids for the expression of M2e fusion proteins to expand the vaccine specificity as reported.[41,42] A flexible linker $(G_4S)_2$ was inserted between M2e and also before and after the whole insert to increase the protein chain flexibility. To construct M2e-inserted FljB-HBc, a forward primer of HBc_{1-149} (5′-GCGCATATGGACATTGACCCGTATAAAG-3′) containing Nde I recognition site (underlined) and a reverse primer (5′-ATAAGCTTTCGTTGTTACTGCTGTATC-3′) reverse complementary to $FljB_{183-191}$ were used to amplify the left portion of FljB-HBc. The forward primer (5′-GATACAGCAGTAACAACGAAAGCTTAT-3′) corresponding to $FljB_{183-191}$ and the reverse primer (5′-GGCATTTTTAGCATCTGCTGAAACAAC-3′) reverse complementary to $FljB_{293-301}$ were used to amplify the synthesized M2e gene flanked with the overlapping sequences from FljB ($FljB_{183-191}$ and $FljB_{293-301}$). The forward primer (5′-GTTGTTTCAGCAGATGCTAAAAATGCC-3′) corresponding to $FljB_{293-301}$ and the reverse primer of HBc_{1-149} (5′-GCGCTCGAGAACAACAGTAGTTTCCGG-3′) containing Xho I recognition site (underlined) were used to amplify the right portion of FljB-HBc. The above three PCR products were mixed at equal molar ratios, and the full-length FH-M2e was amplified using the forward and reverse primers of HBc_{1-149} , as in our previous report.[22] HBc-M2e was constructed using the same strategy by the insertion of four tandem copies of M2e between A80 and S81 of the *adw* subtype of the HBc sequence. The FljB-M2e sequence was amplified from FH-M2e with the forward and reverse primers of FljB, as in our previous report.[22]

For OVA-related plasmid construction, DNA encoding $OVA_{247-274}$ was synthesized by Thermo Fisher Scientific. The flexible linker $(G_4S)_2$ was inserted before and after the $OVA_{247-274}$ sequence. A forward primer of HBc_{1-149} and the reverse primer (5′-GTTTTTCAAAGTTGATTATACTCTCAAGCTGCTCAAGGCCTGAGACTTCATC*ACTACCACCACCACCACTACCACCACCACC*ATAAGCTTTCGTTGTTAC-3′) reverse complementary to a part of the synthesized OVA (underlined), linker (italicized), and $FljB_{186-191}$ (no formatting) were used to amplify the first half of FH-OVA gene. The forward primer (5′-TATAATCAACTTTGAAAAACTGACTGAATGGACCAGTTCTAATGTTATGGAA*GGTGGTGGTGGTAGTGGTGGTGGTGG-TAGT*GTTGTTTCAGCAGATGCT-3′) containing a part of the synthesized OVA (underlined), linker (italicized), and $FljB_{293-298}$ (no formatting) and a reverse primer of HBc_{1-149} were used to amplify the second half of the FH-OVA sequence. The above two PCR products were mixed at 1:1 molar ratio, and the full-length FH-OVA was then amplified with the forward and reverse primers of HBc_{1-149}. HBc-OVA was constructed using the same strategy by insertion of $OVA_{247-274}$ with linkers between A80 and S81 of the *adw* subtype of HBc. The FljB-OVA sequence was amplified from FH-OVA, as described above.

PCR products were purified, digested with Nde I and Xho I, and ligated into the pET-29a vector. Successful ligation was confirmed by sequencing.

Expression, Purification, and Characterization of M2e and OVA Fusion Proteins. Bacterial BL21 cells were transformed with FH-M2e, FljB-M2e, and HBc-M2e plasmids or FH-OVA, FljB-OVA, and HBc-OVA plasmids and grown in LB medium. Recombinant protein expression followed the same procedures as in our recent report.[22] Briefly, IPTG was used to stimulate protein expression, and bacteria pellets were sonicated under native conditions. Supernatants were used to purify FljB-OVA and FljB-M2e, and inclusion bodies were used to purify FH-OVA, HBc-OVA, FH-M2e, and HBc-M2e via Ni-NTA columns. All samples were dialyzed against PBS to initiate protein folding or VLP assembly. Purified proteins were subjected to SDS-PAGE analysis. Samples with putative VLP formation were subjected to TEM and DLS analysis.

Antigen Uptake and DC Maturation. BMDCs were similarly prepared as in our previous report.[43] Immature BMDCs were seeded at 10^6 cells/mL into eight-well chamber slides and stimulated with the FH-M2e VLPs, HBc-M2e, FljB-M2e, and M2e peptide mixture at 70 nM of the respective proteins or peptides. LysoTracker Deep Red (75 nM) was added after 1.5 h to stain acidic organelles. The cells were washed, fixed with 4% paraformaldehyde, and treated with 0.25% Triton X-100 to permeabilize the cell membrane. After washing, the cells were blocked with 2% normal mouse serum in PBS supplemented with 0.1% Tween 20 (PBST) for 1 h at room temperature. The cells were then incubated with 1:200 diluted immune serum from KLH-M2e-immunized mice overnight at 4 °C. After washing with PBST, the cells were incubated with 1:500 diluted AF555-conjugated goat antimouse IgG for 1 h at room temperature. After washing, the chamber wells were removed, and the chamber slides were mounted with antifade fluorescence mounting medium

https://doi.org/10.1021/acsami.2c01028
ACS Appl. Mater. Interfaces XXXX, XXX, XXX−XXX

with DAPI to stain cell nuclei. The cells were imaged under a Nikon Eclipse Ti2 inverted confocal microscope.

For maturation study, immature BMDCs were seeded in 96-well plates and stimulated with the same concentration of FH-M2e VLPs, HBc-M2e, FljB-M2e, and M2e peptides for 20 h. The cells were then stained with fluorescence-conjugated anti-CD11c (N418), anti-CD40 (3/23), anti-CD86 (GL-1), and anti-CD80 (16-10A1) antibodies, followed by flow cytometry analysis in BD FACSVerse.

Immunization. The endotoxin levels of protein samples were reduced to below 7.5 ng/mg for in vivo studies, as in our recent report.[22] For M2e immunization studies, male BALB/c mice were intramuscularly immunized with 40 μg M2e peptide mixture (10 μg/peptide, synthesized by Thermo Fisher Scientific) in the presence of Alum adjuvant (Alhydrogel 2%, Invivogen), 5 μg FljB-M2e, 2.7 μg HBc-M2e, and PBS (first study) or 6.5 μg FH-M2e VLPs, 5 μg FljB-M2e, and PBS (second and third studies). The M2e content remained the same in FljB-M2e, HBc-M2e, and FH-M2e VLP groups, while the M2e peptide mixture contained at least 40 times more M2e content than other groups. For M2e immunization at increased doses, mice were intradermally immunized with 25 μg FljB-M2e or 32.5 μg FH-M2e VLPs (equal M2e content). For M2e immunization involving CpG 1018, mice were intradermally immunized with 24.3 μg FH-M2e VLPs alone or in the presence of 2 μg CpG 1018 or immunized with PBS as a negative control. Immunization was repeated after 3 weeks. For OVA peptide immunization, female C57BL/6 mice were intradermally immunized with 8 μg FH-OVA VLP, 5.8 μg FljB-OVA, 2.6 μg HBc-OVA VLP, or left non-immunized as a negative control. The OVA peptide content remained the same among groups, except for the negative group. For OVA peptide immunization involving CpG 1018, female C57BL/6 mice were intradermally immunized with 8 μg FH-OVA VLPs alone or in the presence of 40 μg CpG 1018 or left non-immunized as a negative control. Immunization was repeated three times at 3-week intervals.

Serum Antibody Titer. Serum anti-OVA or anti-M2e antibody titer was measured by enzyme-linked immunosorbent assay (ELISA) by coating plates with 10 μg/mL $OVA_{247-274}$ peptide (synthesized by GenScript) or 10 μg/mL M2e peptide mixture as in our previous report.[22,44]

Adoptive Transfer and Cell-Mediated Immune Response. Purification of OT-I T cells from OT-I transgenic mice, CFSE staining, and adoptive transfer were performed, referring to our previous report.[45] Mice were then intradermally immunized with different OVA immunogens 24 h after the adoptive transfer of CFSE-stained OT-I T cells. Draining LNs were collected after 4 days, and single-cell suspensions were prepared. In some experiments, cells were stained with fluorescence-conjugated anti-CD4 (GK1.5) and CD8 (53−6.7) antibodies and then subjected to flow cytometry analysis of $CFSE^+$ OT-I T cell expansion. In other experiments, cells were stimulated with the CTL epitope of OVA in the presence of anti-CD28 antibodies overnight. Brefeldin A (420601, Biolegend) was added 5 h before cell harvest. The cells were then stained with fluorescence-conjugated anti-CD8 (53−6.7) antibodies, fixed, and permeabilized and then stained with fluorescence-conjugated anti-Granzyme B (NGZB), TNFα (MP6-XT22), and IFNγ (XMG1.2) antibodies. The percentage of $CFSE^+$ cells in $CD8^+$ T cells and single, dual, and triple cytokine-secreting cells in $CFSE^+$ $CD8^+$ T cells was compared among groups.

Cell-Mediated Immune Response in PBMCs. Isolation, stimulation, and staining of PBMCs to measure the percentage of IL4- and IFNγ-secreting $CD4^+$ and $CD8^+$ T cells were performed, referring to our previous report.[45] In some experiments, cells were stained with fluorescence-conjugated H-$2K^b$-restricted $OVA_{257-264}$ (SIINFEKL) tetramer and anti-CD8 antibodies (53−6.7), both of which were obtained from MBL International. The cells were then fixed, permeabilized, and stained with fluorescence-conjugated anti-Granzyme B (NGZB), TNFα (MP6-XT22), and IFNγ (XMG1.2) antibodies. The cells were subjected to flow cytometry analysis in BD FACSVerse.

Proinflammatory Cytokine and Rectal Temperature. Serum IL-6 and TNFα levels were measured by the mouse IL-6 ELISA kit (88-7604-88, Invitrogen) and mouse TNFα ELISA kit (88-7324-88, Invitrogen), respectively. The mouse rectal temperature was measured right before and 24 h after immunization with a mouse rectal temperature probe connected to PhysioSuite (Kent Scientific).

Influenza Viral Challenge. Influenza viral challenge was performed, referring to our previous report.[44] Briefly, the mice were anesthetized and inoculated intranasally with 4 or 8× LD_{50} PR8, 2× LD_{50} of pdm09, or 5× LD_{50} of H3N2 viruses. Body weight and survival were monitored daily for 14 days. The mice were euthanized and considered dead if their body weight loss was more than 25%.

Tumor Model. E.G7-OVA (CRL-2113, ATCC) and B16F10-OVA cells (a kind gift from Dr. Jeffrey A Hubbell, University of Chicago) were cultured in complete RPMI1640 and DMEM medium, respectively, as in our previous report.[45] Cells were harvested at ∼80% confluency and washed in PBS. BALB/c mice were subcutaneously injected with 10^6 E.G7-OVA cells, and C57BL/6 mice were subcutaneously injected with 10^6 B16F10-OVA cells into the right flank of mice. The tumor size was measured with a digital caliper, and the tumor volume was calculated as in our recent report.[45]

TLR5 Activation Assay. Murine TLR5 activation assay followed the same protocol as in our previous report.[22] Briefly, HEK-Blue mTLR5 cells were seeded into 96-well plates and incubated with FH VLP, FH VLP with D3 domain deleted ($FH_{\Delta D3}$ VLP), FH-OVA VLP, FljB-OVA, and FljB at 8, 40, 200, and 1000 pM for 10 h. OD_{620nm} was read in a microplate reader that reflected the relative TLR5 activation ability.

Statistics. Values were expressed as mean ± SEM (standard error of the mean). Student's t test was used to compare the differences between groups. One-way ANOVA with Tukey's multiple comparison test was used to compare the differences for more than two groups or otherwise specified. P value was calculated by PRISM software (GraphPad, San Diego, CA) and considered significant when it was less than 0.05.

■ ASSOCIATED CONTENT

Supporting Information

The Supporting Information is available free of charge at https://pubs.acs.org/doi/10.1021/acsami.2c01028.

M2e sequences and theoretical molecular weight (MW) of M2e immunogens; FH-M2e VLPs elicit more potent anti-M2e antibody responses than FljB-M2e; rectal temperature change after FljB-M2e and FH-M2e VLP immunization at increased doses; systemic cytokine release after FljB-M2e and FH-M2e VLP immunization at increased doses; OVA peptide sequence and theoretical MW of OVA immunogens; cell-mediated immune responses in PBMCs; antibody responses induced by OVA immunogens; better systemic safety of FH-OVA VLPs as compared to FljB-OVA; comparison of TLR5 activation ability; CpG enhances cell-mediated immune responses induced by FH-OVA VLPs; CpG 1018 potentiates FH-OVA VLP-induced Th1-biased antibody responses; and S12 CpG 1018 (40 μg) slightly increases FH-OVA VLP-induced systemic cytokine release (PDF)

■ AUTHOR INFORMATION

Corresponding Author

Xinyuan Chen − *Biomedical & Pharmaceutical Sciences, College of Pharmacy, University of Rhode Island, Kingston, Rhode Island 02881, United States;* orcid.org/0000-0003-4735-3922; Phone: 401-874-5033; Email: xchen14@uri.edu

https://doi.org/10.1021/acsami.2c01028
ACS Appl. Mater. Interfaces XXXX, XXX, XXX−XXX

Authors

Yiwen Zhao − *Biomedical & Pharmaceutical Sciences, College of Pharmacy, University of Rhode Island, Kingston, Rhode Island 02881, United States*

Zhuofan Li − *Biomedical & Pharmaceutical Sciences, College of Pharmacy, University of Rhode Island, Kingston, Rhode Island 02881, United States*

Jewel Voyer − *Biomedical & Pharmaceutical Sciences, College of Pharmacy, University of Rhode Island, Kingston, Rhode Island 02881, United States*

Yibo Li − *Biomedical & Pharmaceutical Sciences, College of Pharmacy, University of Rhode Island, Kingston, Rhode Island 02881, United States*

Complete contact information is available at: https://pubs.acs.org/10.1021/acsami.2c01028

Author Contributions

X.Y.C. and Y.W.Z. designed the experiments; Y.W.Z., Z.F.L., J.V., and Y.B.L. conducted the experiments and acquired data; X.Y.C. and Y.W.Z. analyzed the data; and X.Y.C. and Y.W.Z. wrote the manuscript.

Notes

The authors declare the following competing financial interest(s): Y.W.Z. and X.Y.C. are inventors of patent applications related to this study. Other authors have no conflict of interests.

The raw/processed data required to reproduce these findings are available from the corresponding author upon request.

■ ACKNOWLEDGMENTS

This work was supported by the National Institutes of Health grants AI139473 and AI156510 (to X.Y.C.). J.V. received support from the URI MARC U*STAR grant from the National Institute of General Medical Sciences of the National Institutes of Health under grant number T34GM131948. The microplate reader and BD FACSVerse used in this work were supported by an Institutional Development Award (IDeA) from the National Institute of General Medical Sciences of the National Institutes of Health grant P20GM103430. TEM images were captured at RI Consortium for Nanoscience and Nanotechnology Lab supported by the National Science Foundation (NSF) EPSCoR Cooperative Agreement #OIA-1655221.

■ REFERENCES

(1) Grgacic, E. V.; Anderson, D. A. Virus-like particles: passport to immune recognition. *Methods* **2006**, *40*, 60−65.

(2) Kushnir, N.; Streatfield, S. J.; Yusibov, V. Virus-like particles as a highly efficient vaccine platform: diversity of targets and production systems and advances in clinical development. *Vaccine* **2012**, *31*, 58−83.

(3) Frietze, K. M.; Peabody, D. S.; Chackerian, B. Engineering virus-like particles as vaccine platforms. *Curr. Opin. Virol.* **2016**, *18*, 44−49.

(4) Laurens, M. B. RTS,S/AS01 vaccine (Mosquirix): an overview. *Hum. Vaccines Immunother.* **2020**, *16*, 480−489.

(5) Gordon, D. M.; McGovern, T. W.; Krzych, U.; Cohen, J. C.; Schneider, I.; LaChance, R.; Heppner, D. G.; Yuan, G.; Hollingdale, M.; Slaoui, M.; Hauser, P.; Voet, P.; Sadoff, J. C.; Ballou, W. R. Safety, immunogenicity, and efficacy of a recombinantly produced Plasmodium falciparum circumsporozoite protein-hepatitis B surface antigen subunit vaccine. *J. Infect. Dis.* **1995**, *171*, 1576−1585.

(6) Roose, K.; De Baets, S.; Schepens, B.; Saelens, X. Hepatitis B core-based virus-like particles to present heterologous epitopes. *Expert Rev. Vaccines* **2013**, *12*, 183−198.

(7) Pumpens, P.; Grens, E. HBV core particles as a carrier for B cell/T cell epitopes. *Intervirology* **2001**, *44*, 98−114.

(8) Nardin, E. H.; Oliveira, G. A.; Calvo-Calle, J. M.; Wetzel, K.; Maier, C.; Birkett, A. J.; Sarpotdar, P.; Corado, M. L.; Thornton, G. B.; Schmidt, A. Phase I testing of a malaria vaccine composed of hepatitis B virus core particles expressing Plasmodium falciparum circumsporozoite epitopes. *Infect. Immun.* **2004**, *72*, 6519−6527.

(9) Oliveira, G. A.; Wetzel, K.; Calvo-Calle, J. M.; Nussenzweig, R.; Schmidt, A.; Birkett, A.; Dubovsky, F.; Tierney, E.; Gleiter, C. H.; Boehmer, G.; Luty, A. J.; Ramharter, M.; Thornton, G. B.; Kremsner, P. G.; Nardin, E. H. Safety and enhanced immunogenicity of a hepatitis B core particle Plasmodium falciparum malaria vaccine formulated in adjuvant Montanide ISA 720 in a phase I trial. *Infect. Immun.* **2005**, *73*, 3587−3597.

(10) Skamel, C.; Ploss, M.; Bottcher, B.; Stehle, T.; Wallich, R.; Simon, M. M.; Nassal, M. Hepatitis B virus capsid-like particles can display the complete, dimeric outer surface protein C and stimulate production of protective antibody responses against Borrelia burgdorferi infection. *J. Biol. Chem.* **2006**, *281*, 17474−17481.

(11) Kratz, P. A.; Bottcher, B.; Nassal, M. Native display of complete foreign protein domains on the surface of hepatitis B virus capsids. *Proc. Natl. Acad. Sci. U. S. A.* **1999**, *96*, 1915−1920.

(12) Mizel, S. B.; Bates, J. T. Flagellin as an adjuvant: cellular mechanisms and potential. *J. Immunol.* **2010**, *185*, 5677−5682.

(13) Hajam, I. A.; Dar, P. A.; Shahnawaz, I.; Jaume, J. C.; Lee, J. H. Bacterial flagellin-a potent immunomodulatory agent. *Exp. Mol. Med.* **2017**, *49*, No. e373.

(14) Smith, K. D.; Andersen-Nissen, E.; Hayashi, F.; Strobe, K.; Bergman, M. A.; Barrett, S. L.; Cookson, B. T.; Aderem, A. Toll-like receptor 5 recognizes a conserved site on flagellin required for protofilament formation and bacterial motility. *Nat. Immunol.* **2003**, *4*, 1247−1253.

(15) Bennett, K. M.; Gorham, R. D., Jr.; Gusti, V.; Trinh, L.; Morikis, D.; Lo, D. D. Hybrid flagellin as a T cell independent vaccine scaffold. *BMC Biotechnol.* **2015**, *15*, 71.

(16) Yang, J.; Zhong, M.; Zhang, Y.; Zhang, E.; Sun, Y.; Cao, Y.; Li, Y.; Zhou, D.; He, B.; Chen, Y.; Yang, Y.; Yu, J.; Yan, H. Antigen replacement of domains D2 and D3 in flagellin promotes mucosal IgA production and attenuates flagellin-induced inflammatory response after intranasal immunization. *Hum. Vaccines Immunother.* **2013**, *9*, 1084−1092.

(17) Song, L.; Zhang, Y.; Yun, N. E.; Poussard, A. L.; Smith, J. N.; Smith, J. K.; Borisevich, V.; Linde, J. J.; Zacks, M. A.; Li, H.; Kavita, U.; Reiserova, L.; Liu, X.; Dumuren, K.; Balasubramanian, B.; Weaver, B.; Parent, J.; Umlauf, S.; Liu, G.; Huleatt, J.; Tussey, L.; Paessler, S. Superior efficacy of a recombinant flagellin:H5N1 HA globular head vaccine is determined by the placement of the globular head within flagellin. *Vaccine* **2009**, *27*, 5875−5884.

(18) Taylor, D. N.; Treanor, J. J.; Sheldon, E. A.; Johnson, C.; Umlauf, S.; Song, L.; Kavita, U.; Liu, G.; Tussey, L.; Ozer, K.; Hofstaetter, T.; Shaw, A. Development of VAX128, a recombinant hemagglutinin (HA) influenza-flagellin fusion vaccine with improved safety and immune response. *Vaccine* **2012**, *30*, 5761−5769.

(19) Turley, C. B.; Rupp, R. E.; Johnson, C.; Taylor, D. N.; Wolfson, J.; Tussey, L.; Kavita, U.; Stanberry, L.; Shaw, A. Safety and immunogenicity of a recombinant M2e-flagellin influenza vaccine (STF2.4xM2e) in healthy adults. *Vaccine* **2011**, *29*, 5145−5152.

(20) Treanor, J. J.; Taylor, D. N.; Tussey, L.; Hay, C.; Nolan, C.; Fitzgerald, T.; Liu, G.; Kavita, U.; Song, L.; Dark, I.; Shaw, A. Safety and immunogenicity of a recombinant hemagglutinin influenza-flagellin fusion vaccine (VAX125) in healthy young adults. *Vaccine* **2010**, *28*, 8268−8274.

(21) Tussey, L.; Strout, C.; Davis, M.; Johnson, C.; Lucksinger, G.; Umlauf, S.; Song, L.; Liu, G.; Abraham, K.; White, C. J. Phase 1 Safety and Immunogenicity Study of a Quadrivalent Seasonal Flu Vaccine Comprising Recombinant Hemagglutinin-Flagellin Fusion Proteins. *Open Forum Infect. Dis.* **2016**, *3*, No. ofw015.

(22) Zhao, Y.; Li, Z.; Zhu, X.; Cao, Y.; Chen, X. Improving immunogenicity and safety of flagellin as vaccine carrier by high-

density display on virus-like particle surface. *Biomaterials* **2020**, *249*, No. 120030.
(23) Mezhenskaya, D.; Isakova-Sivak, I.; Rudenko, L. M2e-based universal influenza vaccines: a historical overview and new approaches to development. *J. Biomed. Sci.* **2019**, *26*, 76.
(24) Deng, L.; Cho, K. J.; Fiers, W.; Saelens, X. M2e-Based Universal Influenza A Vaccines. *Vaccines* **2015**, *3*, 105−136.
(25) De Filette, M.; Min Jou, W.; Birkett, A.; Lyons, K.; Schultz, B.; Tonkyro, A.; Resch, S.; Fiers, W. Universal influenza A vaccine: optimization of M2-based constructs. *Virology* **2005**, *337*, 149−161.
(26) Neirynck, S.; Deroo, T.; Saelens, X.; Vanlandschoot, P.; Jou, W. M.; Fiers, W. A universal influenza A vaccine based on the extracellular domain of the M2 protein. *Nat. Med.* **1999**, *5*, 1157−1163.
(27) Ravin, N. V.; Blokhina, E. A.; Kuprianov, V. V.; Stepanova, L. A.; Shaldjan, A. A.; Kovaleva, A. A.; Tsybalova, L. M.; Skryabin, K. G. Development of a candidate influenza vaccine based on virus-like particles displaying influenza M2e peptide into the immunodominant loop region of hepatitis B core antigen: Insertion of multiple copies of M2e increases immunogenicity and protective efficiency. *Vaccine* **2015**, *33*, 3392−3397.
(28) Kim, M. C.; Song, J. M.; O, E.; Kwon, Y. M.; Lee, Y. J.; Compans, R. W.; Kang, S. M. Virus-like particles containing multiple M2 extracellular domains confer improved cross-protection against various subtypes of influenza virus. *Mol. Ther.* **2013**, *21*, 485−492.
(29) Deng, L.; Mohan, T.; Chang, T. Z.; Gonzalez, G. X.; Wang, Y.; Kwon, Y. M.; Kang, S. M.; Compans, R. W.; Champion, J. A.; Wang, B. Z. Double-layered protein nanoparticles induce broad protection against divergent influenza A viruses. *Nat. Commun.* **2018**, *9*, 359.
(30) Huleatt, J. W.; Nakaar, V.; Desai, P.; Huang, Y.; Hewitt, D.; Jacobs, A.; Tang, J.; McDonald, W.; Song, L.; Evans, R. K.; Umlauf, S.; Tussey, L.; Powell, T. J. Potent immunogenicity and efficacy of a universal influenza vaccine candidate comprising a recombinant fusion protein linking influenza M2e to the TLR5 ligand flagellin. *Vaccine* **2008**, *26*, 201−214.
(31) Armstrong, D. J.; Roman, A. The anomalous electrophoretic behavior of the human papillomavirus type 16 E7 protein is due to the high content of acidic amino acid residues. *Biochem. Biophys. Res. Commun.* **1993**, *192*, 1380−1387.
(32) Alves, V. S.; Pimenta, D. C.; Sattlegger, E.; Castilho, B. A. Biophysical characterization of Gir2, a highly acidic protein of Saccharomyces cerevisiae with anomalous electrophoretic behavior. *Biochem. Biophys. Res. Commun.* **2004**, *314*, 229−234.
(33) Herve, C.; Laupeze, B.; Del Giudice, G.; Didierlaurent, A. M.; Tavares Da Silva, F. The how's and what's of vaccine reactogenicity. *NPJ Vaccines* **2019**, *4*, 39.
(34) Bode, C.; Zhao, G.; Steinhagen, F.; Kinjo, T.; Klinman, D. M. CpG DNA as a vaccine adjuvant. *Expert Rev. Vaccines* **2011**, *10*, 499−511.
(35) Schillie, S. H. A.; Link-Gelles, R.; Romero, J.; Ward, J.; Nelson, N. Recommendations of the Advisory Committee on Immunization Practices for Use of a Hepatitis B Vaccine with a Novel Adjuvant. *MMWR Morb. Mortal. Wkly. Rep.* **2018**, *67*, 455−458.
(36) Abbas, A. K.; Murphy, K. M.; Sher, A. Functional diversity of helper T lymphocytes. *Nature* **1996**, *383*, 787−793.
(37) Krieger, F.; Moglich, A.; Kiefhaber, T. Effect of proline and glycine residues on dynamics and barriers of loop formation in polypeptide chains. *J. Am. Chem. Soc.* **2005**, *127*, 3346−3352.
(38) Talbot, H. K.; Rock, M. T.; Johnson, C.; Tussey, L.; Kavita, U.; Shanker, A.; Shaw, A. R.; Taylor, D. N. Immunopotentiation of trivalent influenza vaccine when given with VAX102, a recombinant influenza M2e vaccine fused to the TLR5 ligand flagellin. *PLoS One* **2010**, *5*, No. e14442.
(39) Xiao, Y.; Liu, F.; Yang, J.; Zhong, M.; Zhang, E.; Li, Y.; Zhou, D.; Cao, Y.; Li, W.; Yu, J.; Yang, Y.; Yan, H. Over-activation of TLR5 signaling by high-dose flagellin induces liver injury in mice. *Cell. Mol. Immunol.* **2015**, *12*, 729−742.
(40) Castell, J. V.; Gomez-Lechon, M. J.; David, M.; Andus, T.; Geiger, T.; Trullenque, R.; Fabra, R.; Heinrich, P. C. Interleukin-6 is the major regulator of acute phase protein synthesis in adult human hepatocytes. *FEBS Lett.* **1989**, *242*, 237−239.
(41) Kim, K. H.; Kwon, Y. M.; Lee, Y. T.; Hwang, H. S.; Kim, M. C.; Ko, E. J.; Wang, B. Z.; Quan, F. S.; Kang, S. M. Virus-like particles presenting flagellin exhibit unique adjuvant effects on eliciting T helper type 1 humoral and cellular immune responses to poor immunogenic influenza virus M2e protein vaccine. *Virology* **2018**, *524*, 172−181.
(42) Deng, L.; Chang, T. Z.; Wang, Y.; Li, S.; Wang, S.; Matsuyama, S.; Yu, G.; Compans, R. W.; Li, J. D.; Prausnitz, M. R.; Champion, J. A.; Wang, B. Z. Heterosubtypic influenza protection elicited by double-layered polypeptide nanoparticles in mice. *Proc. Natl. Acad. Sci. U. S. A.* **2018**, *115*, E7758−E7767.
(43) Chen, X.; Zeng, Q.; Wu, M. X. Improved efficacy of dendritic cell-based immunotherapy by cutaneous laser illumination. *Clin. Cancer Res.* **2012**, *18*, 2240−2249.
(44) Li, Z.; Cao, Y.; Li, Y.; Zhao, Y.; Chen, X. Vaccine delivery alerts innate immune systems for more immunogenic vaccination. *JCI Insight* **2021**, *6*, No. e144627.
(45) Cao, Y.; Zhu, X.; Hossen, M. N.; Kakar, P.; Zhao, Y.; Chen, X. Augmentation of vaccine-induced humoral and cellular immunity by a physical radiofrequency adjuvant. *Nat. Commun.* **2018**, *9*, 3695.

https://doi.org/10.1021/acsami.2c01028
ACS Appl. Mater. Interfaces XXXX, XXX, XXX−XXX